# Power Amplification Efficient Transmitter Structures for Massive MIMO with SC-FDE Schemes: A Promising Combination for 5G Systems?

*Paulo MONTEZUMA*[1,2,3], *Afonso FERREIRA*[1,2], *Rui DINIS*[1,2], *Marko BEKO*[3,4]

[1] Dept. de Engenharia Electrotecnica Faculdade de Ciências e Tecnologia (DEE-FCT), Universidade Nova de Lisboa, Quinta da Torre, 2829-516 Caparica, Portugal
[2] Instituto de Telecomunicações, Instituto Superior Técnico, Av. Rovisco Pais 1, 1049-001 Lisboa, Portugal
[3] UNINOVA, Universidade Nova de Lisboa, Quinta da Torre, 2829-516 Caparica, Portugal
[4] CICANT-CIC.DIGITAL, Universidade Lusófona de Humanidades e Tecnologias, Portugal

pmc@uninova.pt, rdinis@fct.unl.pt

Submitted April 13, 2017 / Accepted November 2, 2017

**Abstract.** *It is well-known that massive multiple-input multiple-output (MIMO) systems have high potential for future wireless broadband systems. Requirements such as high spectral and power efficiency are also crucial in 5G. Based on a multi-amplifier structure it is possible to define a double layered structure where each amplification branch is connected to an antenna array to achieve both constellation and power directivies, assuring at same time similar performances to systems using transmitters with 2-dimensional antenna arrays. Thus, a different path can be followed to improve energy efficiency of power amplification where the usage of parallel amplification branches is combined with big arrays of antennas and multi-stream communication systems. These systems can be combined with single-carrier with frequency domain equalization (SC-FDE) schemes to improve the power efficiency in uplink due to the low envelope fluctuations.*

## Keywords

Massive MIMO, multi-amplifier, power efficiency, double layered structure

## 1. Introduction

High data rate, spectral and energy efficiencies are key requirements for further 5G systems. High data rates can be supported by multiple-input multiple-output systems (MIMO) which can increase throughput with a reduction of the transmitted power by each antenna. With the advent of millimeter waves large numbers of antennas can be deployed in small areas. This allows the use of multiple antenna systems to obtain very high transmission gains, with beamforming and massive MIMO techniques [1–3]. Beamforming is a versatile technique to achieve high data rates [4] in signal transmission in the presence of noise or interference. In practice, the limited number of transmission antennas cannot guarantee perfect directivity, which means that users are still somewhat interfering. Although the design of a beamforming array to maximize the signal power at the intended user is fairly easy, the minimization of the interference is generally a nondeterministic polynomial-time (NP) hard problem [5]. On the other hand, high spectral efficiency requirements are only attainable with the use of multilevel constellations. However, the use of multilevel comes at the expense of reduced power amplification efficiency, which is undesirable in mobile systems [6], [7]. Energy efficiency in power amplification requires the use of nonlinear (NL) amplifiers, which only work with constant or almost constant envelope signals when it is intended to avoid nonlinear distortion.

In this paper the characterization of a new multi-layer transmission system with bi-dimensional antenna arrays is provided. The proposed multi layer-transmitter transmitter combines beamforming with a constellation shaping technique, where multilevel constellations are decomposed into several constant envelope bi-phase shift keying (BPSK) components, that can be amplified separately. The better power amplification efficiency is due to the use of nonlinear amplifiers in such operation [7–9]. Thus, each BPSK component requires a separate radio frequency (RF) chain including a power amplifier. The key difference to MIMO classical implementation relies on the fact that each RF chain is associated to a BPSK component that is combined at channel level to generate the desired multilevel constellation symbol. As we shall see the constellation shaping performed by the transmitter acts as a amplitude and phase distortion of the constellation when the transmitter parameters are unknown. Thus, one might expect that the distortion would affect mutual information (MI) for any user unaware about transmitter configuration. Phase rotations between RF branches lead to

an optimization of the transmitted constellation in a desired direction, but do not have any impact on the directivity of the radiated power, which is only assured by a beamforming operation performed at a different transmitter's layer. The strategy is to blend both techniques in a bi-dimensional antenna array composed by $N_v \times N_h$ antennas, where $N_v$ and $N_h$ are the number of antenna elements aligned vertically and horizontally, respectively. The $N_v$ elements are responsible for the constellation shaping (layer 1) and the $N_h$ elements are responsible for azimuthal radiation directivity (layer 2). For a proper reception, any receiver needs to know the constellation parameters and array configuration used by the transmitter. Consequently, robustness against interception and interference becomes enhanced [10]. This two layer transmit structure is particularly suitable for 5G wireless communications as it can take advantage of the large number of antennas of massive MIMO structures, providing azimuthal power directivity and reinforced physical security against interception.

To cope with the sensitivity to interference of large or non-uniform constellations, specifically intersymbol interference (ISI) caused by multipath propagation and dispersive channel effects, a single-carrier with frequency-domain equalization (SC-FDE) scheme is considered. SC-FDE schemes have also the additional advantage of a lower peak-to-average power ratio (PAPR) when compared with orthogonal frequency-division multiplexing (OFDM).

The main motivation for this paper is to present an extended characterization of this layered transmitter structure combining power efficiency with physical layer security. Section 2 characterizes the concepts behind the multi-layered transmission architecture. Layer 1 configuration possibilities are discussed in Sec. 2.1. The inherent security due to layer 1 is discussed in Sec. 3, being the MI and secrecy capacity analyzed in Sec. 3.1. Receiver's characterization is done in Sec. 4. Methods for transmitter parameters estimation are discussed in Sec. 5, 5.1 and 5.2. Multi-layer implementations are analyzed and evaluated in Sec. 6 and the corresponding simulation results are presented in Sec. 6.1. Finally, Sec. 7 concludes this paper.

## 2. Multiple Layer Architecture

Figure 1 exemplifies the two layered transmission structure, where a massive MIMO scheme is employed with $N_v \times N_h$ antenna elements at the transmitter, arranged in $N_v$ sets of $N_h$ antenna elements. Such as in conventional beamforming schemes $N_h$ antennas are employed to define directive beams for spatial multiplexing purposes and/or interference management as shown in Fig. 1.

Contrarily to MIMO systems, the $N_v$ branches of layer 1 are associated to the constant envelope components in which symbols of multilevel constellations are decomposed. The data bits are mapped into a given constellation (e.g., a quadrature amplitude modulation (QAM) constellation) characterized by the

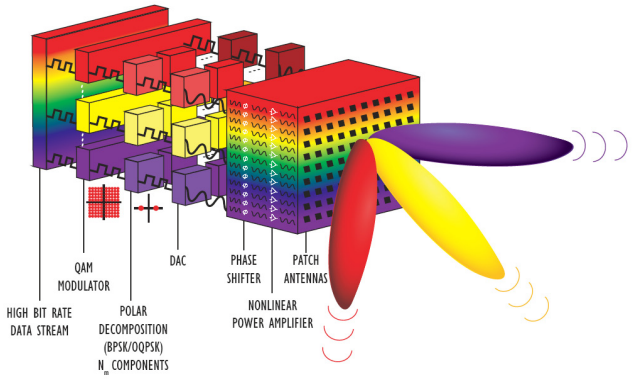


**Fig. 1.** Multi layered transmitter structure.

ordered set $\Im = \{s_0, s_1, \ldots, s_{M-1}\}$ following the rule $(\beta_n^{(\mu-1)}, \beta_n^{(\mu-2)}, \ldots, \beta_n^{(2)}, \beta_n^{(1)}) \mapsto s_n \in \Im$, with $(\beta_n^{(\mu-1)}, \beta_n^{(\mu-2)}, \ldots, \beta_n^{(2)}, \beta_n^{(1)})$ denoting the binary representation of $n$ with $\mu = \log_2(M)$ bits. This means that constellations symbols $x_n$ can be decomposed as a sum of $N_v = \mu$ polar components, i.e.,

$$s_n = g_0 + g_1 b_n^{(1)} + g_2 b_n^{(2)} + g_3 b_n^{(1)} b_n^{(2)} + g_4 b_n^{(3)} + \ldots = \sum_{i=0}^{M-1} g_i \prod_{m=0}^{\mu-1} \left(b_n^{(m)}\right)^{\gamma_{m,i}} = \sum_{i=0}^{M-1} g_i b_n^{eq(i)}, \quad (1)$$

with $(\gamma_{\mu,i}\ \gamma_{\mu-1,i}\ \ldots\ \gamma_{2,i}\ \gamma_{1,i})$ denoting the binary representation of $i$, $b_n^{eq(i)} = \prod_{m=0}^{\mu-1} \left(b_n^{(m)}\right)^{\gamma_{m,i}}$ and $b_n^{(m)} = (-1)^{\beta_n^{(m)}}$ is the polar representation of the bit $\beta_n^{(m)}$. Since we have $M$ constellation symbols in $\Im$ and $M$ complex coefficients $g_i$, eq. (1) can be used to define a system of $M$ equations to obtain the coefficients $g_i$, $i = 0, 1, \ldots, M-1$ [11]. If we assume $N_v$ as the number of non-null coefficients $g_i = |g_i| \exp(j\theta_i)$, then a given constellation symbol can be decomposed as a sum of $N_v \leq M$ polar components. Each one of the $N_v$ polar components is modulated as a BPSK signal (or other polar modulation format with constant envelope), that can be a serial representation of an offset quadrature shift keying (OQPSK) signal [12], with reduced envelope fluctuations and compact spectrum (e.g., a gaussian minimum shift keying (GMSK)). These signals are separately amplified by a nonlinear amplifier before being transmitted by the $N_v$ arrays of $N_h$ antennas.

Due to phase shifts between the $N_v$ antenna arrays (associated to the amplification branches), it is possible to rearrange the symbols according to a desired direction $\Phi$ (under these conditions the constellation's shaping in the desired direction is assured by phase rotations of the BPSK components). This means that directivity at the information level is achieved, as the constellation shape is modified according the direction $\Phi$. Furthermore, security is achieved since the $g_i$ coefficients are only known by the transmitter and the intended receiver. It is important to mention that there is no beamforming due to layer 1 since the $N_v$ antennas transmit uncorrelated signals and phase variations between RF

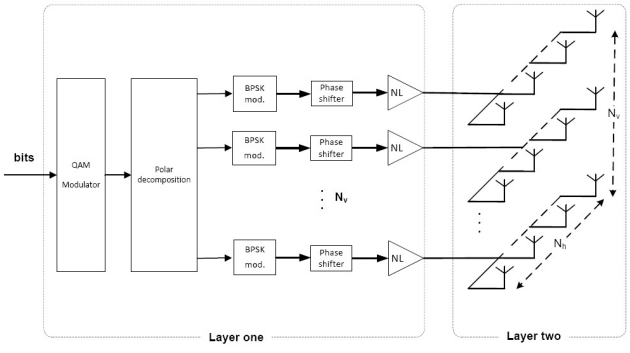


**Fig. 2.** Proposed double layer transmitter structure.

branches do not have any impact on the azimuthal radiation pattern. Changes in radiation pattern are only due to the $N_\mathrm{h}$ antennas of layer 2.

For example, the transmitter structure associated to a 16-QAM and 64-QAM constellation has $N_\mathrm{v} = 4$ and $N_\mathrm{v} = 6$, respectively. Each amplification one of the $N_\mathrm{v}$ branches is connected to an antenna array of layer 2 with $N_\mathrm{h}$ antennas. In this layer all the $N_\mathrm{h}$ antenna elements are employed to define directive radiation beams for spatial multiplexing purposes as shown in Fig. 2.

### 2.1 Layer 1 Configuration Possibilities

As stated before (1) can be used to describe several mapping rules of M-QAM and Voronoi constellations [13]. For instance, the definition of a 64-QAM constellation with Gray mapping only needs 6 non-null $g_i$ coefficients: $g_4 = 4$, $g_6 = 2$, $g_7 = 1$, $g_{32} = 4\mathrm{j}$, $g_{48} = 2\mathrm{j}$ and $g_{56} = \mathrm{j}$. 16-QAM constellations with Gray mapping are the sum of 4 BPSK signals defined in terms of the set of non-zero complex coefficients $g_2 = 2\mathrm{j}$, $g_3 = \mathrm{j}$, $g_8 = 2$ and $g_{12} = 1$ (actually, this corresponds to only two QPSK constellations). Other mapping rules or constellations can be easily obtained by changing the set of coefficients $g_i$ (for example, energy optimized 16 and 64 Voronoi constellations are characterized by 15 and 63 non-null complex coefficients $g_i$). For the particular case of $M$-ary constellations there are $M!$ possible mappings, which makes impractical for the eavesdropper to decode when transmissions are based on constellations with sizes equal or greater than 64 (this option is similar to schemes where physical layer security is ensured through constellation diversity). In this paper we do not explore the potential of mapping diversity since we restrict current analysis to the security assured by layer 1's constellation shaping. This means that in every transmission the transmitter uses a custom constellation mapping, which may act as a secret key to any interception from a eavesdropper.

Another factor that also increases the complexity associated to any interception relies on the configuration possibilities of the transmitter array, since the arrangement of the coefficients $g_i$ among the transmit antennas can be changed. Being the number of active antennas the same as of BPSK components, i. e., $N_\mathrm{v}$ components, for each mapping rule and uniform array configuration there are $N_\mathrm{v}^{N_\mathrm{v}} - N_\mathrm{v}$ different array configurations. This also means that we have the same number of different spatial arrangements for the constellation symbols. Thus, combining both mapping possibilities and $g_i$ permutations between antennas, for any interception the eavesdropper needs to compute $N_\mathrm{v}! \times N_\mathrm{v}^{N_\mathrm{v}} - N_\mathrm{v}$ combinations.

The complexity can be even increased through resort to non-uniform spacing between branches of layer 1. Consider the transmitter structure of Fig. 2 with equally spaced $N_a = 16$ single antennas, where only 4 are active in each instant. In this case the active antennas can be any set of $N_\mathrm{v} = 4$ antennas among $\frac{N_a!}{N_a - N_\mathrm{v}}$ possible combinations. Obviously, this situation does not reflect the real number of possibilities, since the spacing between antennas can be any real multiple of $\lambda$, leading to a phase shift between antennas $\Delta\theta \in [0, 2\pi]$. Despite this fact, simulation results presented here are restricted to the transmitter's configurations where the spacings are an integer multiple of $d$, with $d = \lambda/2$.

Only for analysis purposes of layer 1, and if nothing is said in contrary, the uniform arrangements of BPSK components along the $N_\mathrm{v}$ RF branches for 16-QAM and 64-QAM are 2j, 1, 2, j and 2j, 1, 2, j, 4j, 4, respectively.

## 3. Impact on Security

As stated before a regular $M$-QAM constellation may be expressed as a sum of M polar components. Let us assume $N_\mathrm{v}$ antennas equally spaced by $d$. In such conditions, in each branch $i$ the polar components $g_i b_n^{eq(i)} = |g_i|\mathrm{e}^{\varphi_i}\mathrm{e}^{\theta_i} = |g_i|\mathrm{e}^{\varrho_i}$, with $\varphi_i = \pm\pi, \pm\pi/2$, are affected by a phase rotation of $\alpha_i = 2\pi(i-1)d/\lambda \cos\left(\frac{\pi}{2} + \phi\right)$ and the transmitted symbol is given by

$$x = \sum_{i=1}^{N_\mathrm{v}} |g_i|\mathrm{e}^{\varrho_i} \exp(\alpha_i) = \sum_{i=1}^{N_\mathrm{v}} |g_i|\mathrm{e}^{\phi_i}. \tag{2}$$

From (4), becomes obvious that each polar component suffers a different rotation that depends on the antenna position and sort order adopted along the $N_\mathrm{v}$ branches. Hence, the shaping of the constellation acts as a nonlinear distortion when unknown by the receiver. Under these conditions the user sees a nonlinear channel with additive noise, described by

$$Y = f_a(x) + N \tag{3}$$

where $f_a(x) = k_a x \mathrm{e}^{\mathrm{j}\alpha_a}$, with $k_a$ and $\alpha_a$ denoting the AM/AM and AM/PM characteristic, respectively. This means that When the knowledge of the coefficients $g_i$ is not available, the distortion effects on the transmitted constellation are comparable to nonlinear distortion introduced by a nonlinear channel with an AM/AM and an AM/PM non-null characteristic.

Let us consider the 16-QAM defined by $N_\mathrm{v} = 4$ components, where half are associated to the in-phase component

and other two to the quadrature component and characterized by the symbol given by $|g_1|\cos(\varrho_1) + |g_2|\cos(\varrho_2) + \mathrm{j}(|g_1|\sin(\varrho_1) + |g_2|\sin(\varrho_2))$. Assuming $\alpha_i = 0$ for the first antenna, due to the array configuration the transmitted symbol is given by

$$x' = |g_1|\cos(\varrho_1) + |g_2|\cos(\varrho_2 + \alpha_2) + \mathrm{j}(|g_1|\sin(\varrho_1) + |g_2|\sin(\varrho_2 + \alpha_2)) = K_a x \mathrm{e}^{(\mathrm{j}\alpha_a)} \quad (4)$$

where $K_a$ and $\alpha_a$ can be viewed as an amplitude and a phase distortion, respectively.

When the $g_i$ coefficients and the arrangements of the components over the amplification branches are unknown the resulting transmitted symbol can be viewed as composed of the sum of several random sinusoidal vectors. This means that we have a mathematical problem characterized by the existence of $N_\mathrm{v} = \log_2(M)$ vectors with lengths $A_i = |g_i|$ and angles $\phi_i$, where $A_i$ and $\phi_i$ are random variables (although, we are assuming that the number of components is known). Under these conditions we may describe the resultant vector as

$$A\mathrm{e}^{(\mathrm{j}\Phi)} = \sum_{i=1}^{N_\mathrm{v}} |g_i|\mathrm{e}^{(\mathrm{j}\phi_i)} = x_\mathrm{R} + \mathrm{j}x_\mathrm{I}. \quad (5)$$

We may also assume:

- amplitude $A_i$ and angle $\phi_i$ of the $i^{\text{th}}$ elementary phasor are statically independent of each other and of the amplitudes and phases of all other vectors;
- the random variables $A_i$'s are identically distributed for all $i$, with mean $\overline{A}$ and moment $\overline{A}^2$;
- the phases $\phi_i$ are all uniformly distributed on $[-\pi, \pi]$.

Due to central limit theorem, for large values of $\log_2(M)$ both $x_\mathrm{R}$ and $x_\mathrm{I}$ will be approximately Gaussian (this means that constellations decomposed by a higher number of components have advantage over the smaller ones). It follows that this Gaussian approach will be more exact for energy efficient constellations such as Voronoi that are decomposed in terms of $M - 1$ components. Let us assume that the last two conditions are relaxed. Under these conditions the real $X$ and imaginary $Y$ parts can be defined as

$$x_\mathrm{R} = \mathrm{Re}(A\exp(\mathrm{j}\Phi)) = \sum_{i=1}^{N_\mathrm{v}} |g_i|\cos(\phi_i), \quad (6)$$

and

$$x_\mathrm{I} = \mathrm{Im}(A\exp(\mathrm{j}\Phi)) = \sum_{i=1}^{N_\mathrm{v}} |g_i|\sin(\phi_i). \quad (7)$$

With variances

$$\sigma^2_{x_\mathrm{R}} = E[x_\mathrm{R}^2] = \sum_{n=1}^{N_\mathrm{v}}\sum_{m=1}^{N_\mathrm{v}} E[|g_n g_m|]E[\frac{1}{2} + \frac{1}{2}\cos(2\phi_n)] \quad (8)$$

and

$$\sigma^2_{x_\mathrm{I}} = E[x_\mathrm{I}^2] = \sum_{n=1}^{N_\mathrm{v}}\sum_{m=1}^{N_\mathrm{v}} E[|g_n g_m|]E[\frac{1}{2} + \frac{1}{2}\sin(2\phi_n)], \quad (9)$$

since for $n \neq m$, $E[\cos(\phi_n)\cos(\phi_m)] = E[\cos(\phi_n)]E[\cos(\phi_m)] = 0$ , where $E$ denotes the expectation and likewise we have $E[\sin(\phi_n)\sin(\phi_m)] = E[\sin(\phi_n)]E[\sin(\phi_m)] = 0$. If $\phi_n$ is uniformly distributed on $(-\pi, \pi)$ results $\sigma^2_{x_\mathrm{R}} = \sum_{m=1}^{N_\mathrm{v}} E[|g_n^2|]$ and $\sigma^2_{x_\mathrm{I}} = \sum_{m=1}^{N_\mathrm{v}} E[|g_n^2|]$, which means that both variances are identical.

The simplest case is the transmitter based on the decomposition of the M-QAM, with $N_\mathrm{v}/2$ in-phase components and $N_\mathrm{v}/2$ quadrature components. Let assume that only phase shifts in the transmitter array affecting the components with lower amplitude are unknown. In such conditions the resultant vector associated to each component can be viewed as the sum of a constant phasor and a random phasor. Let us consider the in-phase component. For the sake of simplicity, it is assumed that the known phasor of the in-phase component lies in the real axis. Thus, the real and imaginary parts of the resultant phasor will be given by

$$x_\mathrm{R} = \mathrm{Re}(A\exp(\mathrm{j}\Phi)) = |A_0| + \sum_{n=1}^{N_\mathrm{v}/2-1} |g_n|\cos(\phi_n) \quad (10)$$

and

$$x_\mathrm{I} = \mathrm{Im}(A\exp(\mathrm{j}\Phi)) = \sum_{n=1}^{N_\mathrm{v}/2-1} g_n\sin(\phi_n) \quad (11)$$

where $A_0$ denotes the length of the known phasor. It becomes obvious that the effect of the known phasor is to add a mean value to the real part of the resultant phasor. When we have a large number of random contributions, the statistics of the real and imaginary parts of the resultant vector are asymptotically Gaussian, with joint probability density function (PDF) given by

$$P_{\mathrm{R,I}}(x_\mathrm{R}, x_\mathrm{I}) = \frac{1}{2\pi\sigma^2}\mathrm{e}^{-\frac{((x_\mathrm{I}-A_0)^2+x_\mathrm{I}^2)}{2\sigma^2}}. \quad (12)$$

Since $A = \sqrt{x_\mathrm{R}^2 + x_\mathrm{I}^2}$ and $\theta = \arctan(x_\mathrm{I}/x_\mathrm{R})$ we may write (12) as

$$P_{A,\theta}(A, \theta) = \frac{A}{2\pi\sigma^2}\mathrm{e}^{-\frac{(A^2+A_0^2-2AA_0\cos(\theta))}{2\sigma^2}}. \quad (13)$$

Based on (13) it is easy to conclude that the pdf of $A$ follows a "Rician" density function given by

$$P_A(A) = \frac{A}{\sigma^2}\mathrm{e}^{(-\frac{A^2+A_0^2}{2\sigma^2})}J_0(\frac{AA_0}{\sigma^2}) \quad (14)$$

where $J_0$ represents a hyperbolic Bessel function of the first kind [14]. Thus, for an eavesdropper the lack of information about transmitter's configuration, means that the received symbol will be the combination of real and imaginary parts that have a "Rician" PDF. For example, for a 16-QAM the sum of two in-phase components with amplitudes 1 and 2 and unknown phases uniform distributed on $[-\pi, \pi]$ has the result of Fig. 3. Obviously, the quadrature component will have the same behavior. In such conditions, the eavesdropper sees a constellation totally corrupted by the phase rotations, being impossible to demodulate the received signals. Obviously, when the size of the constellation grows the number of polar

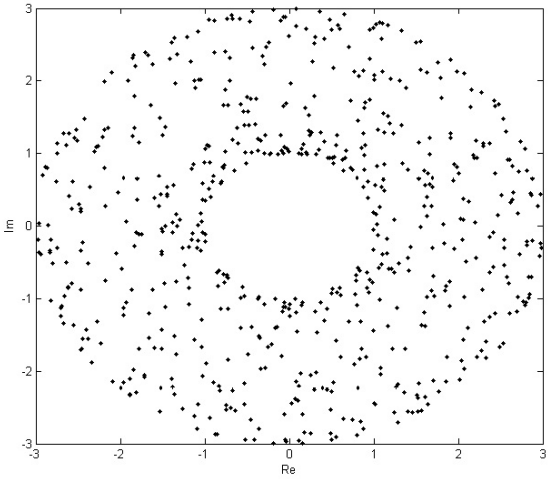


**Fig. 3.** Effect of phase uncertainty in the sum of two in-phase components for 16-QAM.

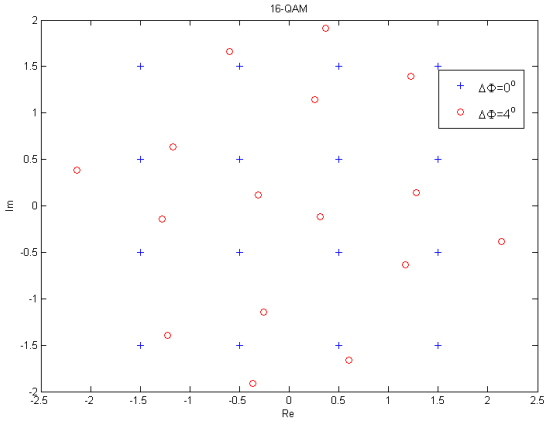


**Fig. 4.** 16-QAM:Effect of an error ΔΦ in the received constellation.

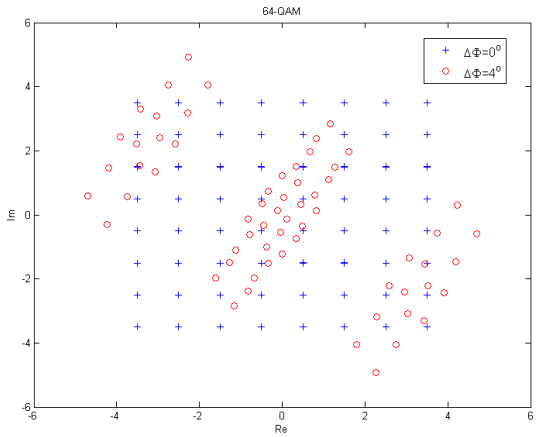


**Fig. 5.** 64-QAM:Effect of an error ΔΦ in the received constellation.

components involved in the definition of each symbol also grows and the area of uncertainty will be larger. Moreover, even when the errors due to phase incertitude associated to each component are small these errors may have a strong distortion effect in the resulting symbol (since the symbol results from the combination of components). This effect is shown in Fig. 4 and 5, where it can be seen the distortion effect in the constellation due to small errors on the estimation of transmitter parameters that lead to an incorrect estimation of $\Phi' = \Phi + \Delta\Phi$ (it is assumed that the constellation optimized under $\Phi$ is a regular $M$-QAM).

In view of the above, it is clear the potential of the proposed transmitter structure to support a physical layer scheme. However, physical layer security shall not affect the ability of authorized users to decode data. Next section presents an analysis of the level of security provided by these type of transmitter structures, in which it is demonstrated that, despite the security, the decoding capacity of authorized users remains practically unchanged.

## 3.1 Mutual Information and Secrecy

Let us assume that $x(t)$ denotes the $n$th transmitted symbol associated to a given block by

$$x(t) = s_n h_T(t - nT_S) \tag{15}$$

where $T_S$ represents the symbol duration and $h_T(t)$ denotes the adopted pulse shape. $s_n$ belongs to a given size-$M$ constellation $\mathfrak{S}$. Under these conditions the received signals by the authorized receiver and the eavesdropper are

$$y(t) = f_a(x(t)) + n_1(t) \tag{16}$$

and

$$z(t) = f_a(x(t)) + n_2(t), \tag{17}$$

with $n_1(t)$ and $n_2(t)$ denoting de noise terms and $f_A(.)$ denotes the shaping performed by layer 1. Perfect secrecy means that $I(X;Z) = 0$, with $X$ the sent message and $Z$ the received message by the eavesdropper and where $I(;)$ denotes the MI. It should be noted that the MI (assuming equiprobable symbols) for a given signal set $\mathfrak{S}$ [15], can be written as

$$I(X,Y) = \log_2 M - \frac{1}{M}\sum_{s\in\mathfrak{S}} E_n\left[\log_2 \chi\right] \tag{18}$$

where $\chi = \sum_{s'_n\in\mathfrak{S}} \exp(-\frac{1}{N_0}|\sqrt{Es}(x_n - x'_n) + n|^2 - |n|^2)$. Expressing the secrecy capacity in terms of the MI we may write

$$C_s = \max_{s\in F}\left[I(X;Y) - I(X;Z)\right] \tag{19}$$

where $F$ denotes the set of all PDFs at the channel input under power constraint at the transmitter, $I(X;Y)$ denotes the MI of the intended receiver and $I(X;Z)$ represents the MI of eavesdropper.

With the purpose of evaluating the influence of layer 1 in physical layer security we consider an AWGN channel and it is assumed that the authorized receiver knows the set of coefficients $g_i$ and $f_a(.)$. Symbols $s_n$ are selected with equal probability from a $M$-QAM constellation (dimensions of $M = 16$ and $M = 64$ are considered).

| 16QAM | Antenna order | | | |
|---|---|---|---|---|
| | 1 | 2 | 3 | 4 |
| Coefficients $g_i$ | 2j | 1 | 2 | j |
| Spacings | | 4d | 8d | 10d |
| | | 4d | 8d | 11d |

**Tab. 1.** 16-QAM: Arrangement of the coefficients $g_i$ by the antennas and the spacings to first antenna.

| 64QAM | Cases | Antenna order | | | | | |
|---|---|---|---|---|---|---|---|
| | | 1 | 2 | 3 | 4 | 5 | 6 |
| Coefficients $g_i$ | | 2j | 1 | 2 | j | 4 | 4j |
| Spacings | A | 1d | 6d | 9d | 18d | 25d | 27d |
| | B | 1d | 6d | 9d | 18d | 20d | 27d |
| | C | 1d | 6d | 9d | 16d | 25d | 27d |
| | D | 1d | 6d | 9d | 16d | 18d | 27d |

**Tab. 2.** 64-QAM: Arrangement of the coefficients $g_i$ by the antennas and spacings to first antenna.

It is assumed linear power amplification at the transmitter and perfect synchronization. Two options are considered regarding the antenna arrangement of layer 1: in the first one antennas are equal spaced by $d/\lambda = 1/4$ and in the second one the arrangement between antennas can be non-uniform. For uniform arrangements 24 permutations were analyzed for 16-QAM and 720 permutations were considered for 64-QAM. Also, a total of 1024 non-uniform antenna arrangements were tested. From the set of tested arrangements it became clear that the MI results for the authorized receiver are largely unaffected by changes on antennas permutations. On the other hand, for the eavesdropper the MI values were always null even when the $g_i$ values were known without the information regarding the array configuration, which means a secrecy capacity of one hundred percent.

Thus, the results presented here are those that best reflect the behavior of the MI among the tested arrangement. For uniform arrays the components have the antennas' arrangements presented in Tab. 1 and 2 but with equally spaced antennas. The corresponding non-uniform arrangements and spacings are those presented in Tab. 1 and 2, respectively. The results refer to the behavior of MI with the optimization angle $\Phi$ for a fixed signal to noise ratio (SNR) (14 dB for 16-QAM and 16 dB for 64-QAM).

Figure 6 shows the MI evolution with angle $\Phi$, for transmitters based on constellations 16-QAM and 64-QAM with uniform arrays. It is clear that MI is practically unaffected by the optimization angle in which the constellation is configured. Hence, we may concluded that independently of the direction in which the constellation is optimized, a receiver aware about the transmitter's configuration will be able to decode with success the transmitted information. However, the MI values have a minimum at 60°, which means that angles near $\Phi \simeq 60°$ should be avoided, otherwise the system's performance can be compromised. As expected 64-QAM has more minimums than 16-QAM. It is important to mention that the number of minima increases with the number of polar components, which means an increased secrecy capacity since the transmitter can be optimized for an angle in

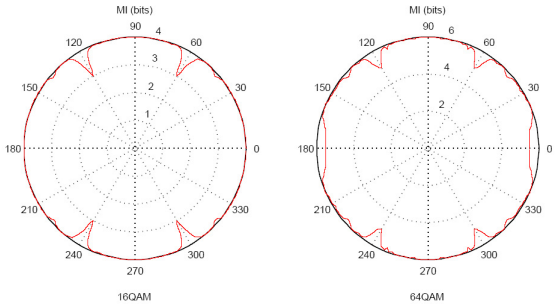


**Fig. 6.** MI behavior with the angle $\Phi$ for uniform spacing between antennas.

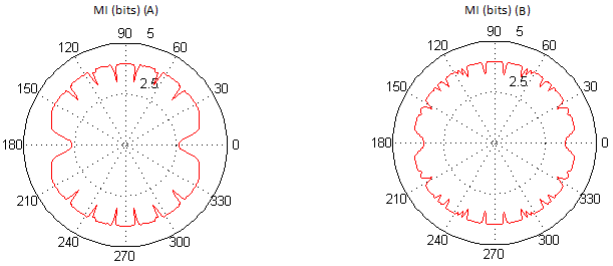


**Fig. 7.** MI behavior with the angle $\Phi$ for non-uniform spacing between antennas and 16-QAM.

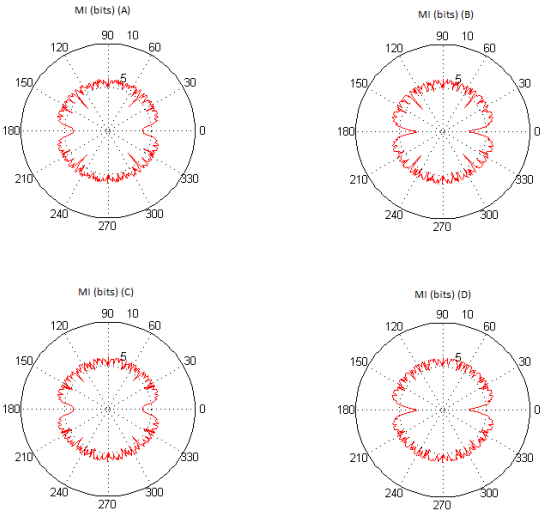


**Fig. 8.** MI behavior with the angle $\Phi$ for non-uniform spacing between antennas and 64-QAM.

the vicinity of these minima, compromising any interception based on a coarse estimation of the transmission parameters.

A similar behavior can be seen in Fig. 7 and 8 regarding non-uniform arrays (sub-plots A, B, C and D in Fig. 8 refer the same cases of Tab. 2). Now due to non-uniform arrangement the number of minima increases for both constellation sizes, but for the majority of the angles $\Phi$ the MI values for any authorized receiver are practically unaffected by changes on non-uniform arrangements. From previous results it can be foreseen a higher impact of estimation errors of angle $\Phi$ on the performance of systems using non-uniform arrays.

It becomes obvious that the eavesdropper needs to know the arrangement of $g_i$ among the amplification branches as well the antenna spacing. However, this is not a realistic supposition having in mind previous considerations about the number of possible configurations. It should be mentioned that there is a secrecy level of hundred percent when the set of coefficients $g_i$ and the array arrangement are unknown (in this case we have a null value for MI).

It is also convenient to mention that a method for physical layer security was proposed in [16] based on random phase rotations of the sub-constellations in which each constellation can be decomposed. Obviously, the random phase rotations affecting the each sub-constellation have the same effect of the phase rotations due to the array configuration of the transmitted structure considered here. Moreover, the decompositions into QPSK components and BPSK components are equivalent the impact of the lack of knowledge about the value of the phase rotations can be treated in the same way as in [16], reason why the same theoretical analysis and expressions for the symbol error rate (SER) and bit error rate (BER) presented in [16] are valid here.

# 4. Receivers Characterization - Single User Scenario

As referred previously in Sec. 1, to cope with channel's frequency selectivity an iterative block decision feedback equalization (IB-DFE) receiver whose structure is depicted in Fig. 9 [17], [18] is adopted. As usual, the cyclic prefix corresponds to a periodic extension of the useful part of the block with size $N$, i.e., $x_{-n} = x_{N-n}$ with a length higher than the overall channel impulse response.

Since the samples associated to the cyclic prefix are discarded by the receiver, we have null inter block interference (IBI) and the impact of a time-dispersive channel is equivalent to a scaling factor for each frequency. Thus, the corresponding frequency-domain block $\{Y_k; k = 0, 1, \ldots, N-1\}$ is the discrete Fourier transform (DFT) of the time-domain block $\{y_n; n = 0, 1, \ldots, N-1\}$, and can be described as

$$Y_k = X_k H_k + z_k, \tag{20}$$

with $H_k$ denoting the channel frequency response for the $k^{\text{th}}$ subcarrier and $z_k$ the corresponding AWGN.

After first iteration the data symbols obtained from the IDFT are given by

$$\tilde{\mathbf{X}}_k = \left(\mathbf{H}_k \mathbf{H}_k^{\mathrm{H}} + \alpha \mathbf{I}\right)^{-1} \mathbf{H}_k^{\mathrm{H}} \mathbf{Y}_k \tag{21}$$

and

$$\tilde{\mathbf{X}}_k^i = \left((1-(\rho^{i-1})^2)\mathbf{H}_k \mathbf{H}_k^{\mathrm{H}} + \alpha \mathbf{I}\right)^{-1} \mathbf{H}_k^{\mathrm{H}} \mathbf{Y}_k - \mathbf{B}_k^{(i)} \overline{\mathbf{X}}_k^{(i-1)}, \tag{22}$$

for the subsequent iterations, with $\overline{X}_k$ denoting the frequency-domain average values conditioned to the FDE output for the previous iteration, which can be computed as described in [19], and $\{F_k; k = 0, 1, \ldots, N-1\}$ and $\{B_k; k = 0, 1, \ldots, N-1\}$ given by

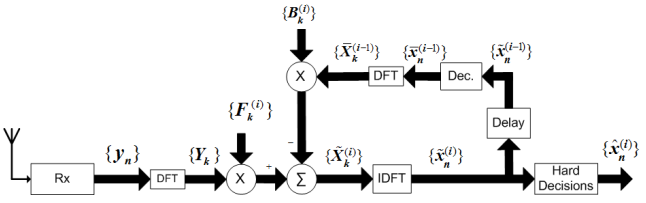


**Fig. 9.** IB-DFE receiver with soft decisions.

$$\mathbf{F}_k^i = \frac{\kappa \mathbf{H}_k^{\mathrm{H}}}{\alpha \mathbf{I} + (1-(\rho^{i-1})^2)\mathbf{H}_k \mathbf{H}_k^{\mathrm{H}}} \tag{23}$$

and

$$\mathbf{B}_k^i = \mathbf{F}_k^i \mathbf{H}_k - \mathbf{I}, \tag{24}$$

denote the feedforward and the feedback coefficients, respectively [11], [20]. For each channel $\alpha = E[|N_k|^2]/E[|X_k|^2]$ and $\kappa$ is normalization factor to ensure that $\sum_{k=0}^{N-1} F_k H_k / N = 1$. The correlation coefficient $\rho$ can be regarded as a measure of the reliability of the decisions employed in the feedback loop and can be computed as described in [11], [20].

To have an idea of the impact of the information directivity in the system performance, Fig. 10 and 11 present a set of BER results over fading channels (the matched filter bound (MFB) is also included for comparison purposes). We consider a SC-FDE modulation with blocks of $N = 256$ useful symbols and a cyclic prefix of 32 symbols longer than overall delay spread of the channel. The modulation symbols belong to a $M$-QAM or Voronoi constellation (with $M = 16$ or $M = 64$) and are selected from the transmitted data according to a mapping rule that optimizes energy efficiency. The severely time-dispersive channel is characterized by an uniform power delay profile (PDP), with 32 equal-power taps, and uncorrelated Rayleigh fading on each tap. It is also assumed an uniform array with equally spaced antennas with $d/\lambda = 1/4$ and the coefficients $g_i$ follow the sort order of tables 1 and 2, respectively. Performance results are expressed as function of $\frac{E_b}{N_0}$, where the $N_0$ is the one-sided power spectral density of the noise and $E_b$ represents the energy of the transmitted bits.

As expected these results confirm previous results regarding the MI evolution. Again the constellations with higher dimensions are more sensitive to angle errors $\Delta\Phi$ relative to the transmission direction $\Phi$. The reason for that lies in the higher number of MI's minima due to the higher number of uncorrelated BPSK components. Clearly, the Voronoi constellations have an higher information directivity because they are decomposed in more polar components and consequently use more RF branches. Obviously, this lead to a system more sensitive to $\Phi$ and makes them a good choice to increase directivity and reduce interference or the probability of communication interception. Yet, security can be always increased by encryption techniques [21–23]. Despite these facts, it is clear that the performance remains

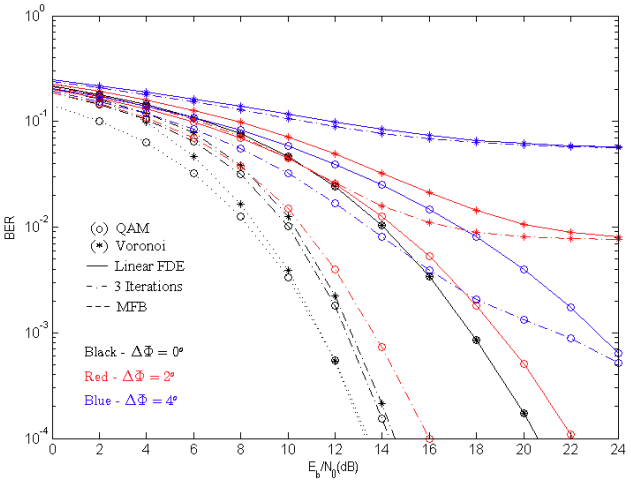


**Fig. 10.** BER performance for both configuration options.

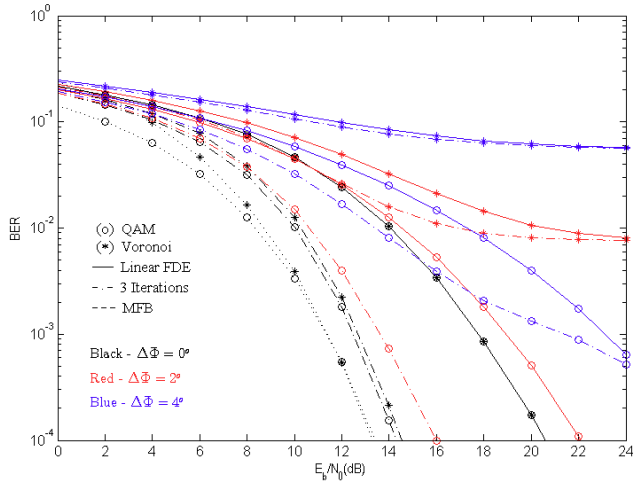


**Fig. 11.** BER performance for both configuration options.

unaffected when no error occurs on the estimation of Φ (best performance results are close to MFB), and this is valid for both types of constellations, regardless of size. This means that constellation shaping of layer 1 can be used without negative impact on system performance, provided that the receiver knows transmitter's configuration.

Previous results have shown the high sensitivity of the BER against any error on the estimation of Φ for an eavesdropper or any authorized receiver unable to estimate exactly the transmitter's parameters that lead to the constellation shape optimized for Φ. However, it is not realistic to assume that eavesdropper knows in advance the initial configuration of the transmitter, including the coefficients $g_i$, the arrangement of these coefficients in the several RF branches and the spacing between antennas. Results also showed that non-uniform arrays outperform the security achieved by the uniform ones, due to the lower tolerance against any estimation error. This low tolerance, together with the complexity, means that the computational load associated to any interception can be prohibitive (the same conclusion is still valid for uniform configurations). Additional increases on security can be achieved by changing dynamically the configuration of coefficients $g_i$ between successive transmitted blocks according to a pattern known by the transmitter and the intended user.

But now two questions arise:

- how to compute the transmitter parameters efficiently?
- will have the combination of the power efficient amplification structure of layer 1 any impact on system performance when combined with layer 2?

In the following we will try answer to these two questions.

# 5. Parameters Estimation

Channel variations or synchronization problems between the RF circuits may cause phase and gain imbalances. One way to compensate possible effects of these imperfections on the transmitter is to apply estimation techniques for $g_i$ based on pilots. These techniques can use least squares (LS) or minimum square error (MMSE) estimators. Typically, channel estimation is performed by sending a set of symbols known by the receiver, which are sent in each block of transmitted symbols [24–26]. However, the channel estimation using pilots is outside the scope of the present work, since it is assumed perfect channel state information (CSI). So the current analysis is restricted to the estimation problem of the coefficients $g_i$, through the use of pilots. In the following, a method for estimating the $g_i$ coefficients for a transmitter based on a 16-QAM is characterized. The method can be easily extended to other types of constellations such as 64-QAM or Voronoi. Another estimation method with similar complexity and performance was proposed in [27].

## 5.1 Estimation Based on Pilots

Let us consider a regular 16-QAM, characterized by the set of coefficients ±1, ±2, ±j and ±2j. For the estimation of the constellation only a set of 5 pilots $P1$, $P2$, $P4$, $P7$ and $P8$ belonging to the constellation is needed, provided that this set of symbols encompasses all of the components $g_i$ used in the construction of the constellation symbols. It should be noted that the subset of symbols used as pilots may be another, provided that all $g_i$ are used in their definition (for example, for 64-QAM, at least 6 different pilots are required to cover all $g_i$). Thus, the reference pilots may have the values shown in Tab. 3.

| 16-QAM | Antennas | | | | Reference pilots |
|---|---|---|---|---|---|
| Coefficients $g_i$ | 2j | 1 | 2 | j | |
| P1 | 2j + j | + 1 | + 2 | | 3j + 3 |
| P2 | 2j + j | − 1 | + 2 | | 3j + 1 |
| P3 | 2j − j | − 1 | + 2 | | j + 1 |
| P4 | 2j − j | + 1 | + 2 | | j + 3 |
| P5 | 2j − j | + 1 | − 2 | | j − 1 |
| P6 | −2j + j | + 1 | − 2 | | −j − 1 |
| P7 | 2j + j | + 1 | − 2 | | 3j − 1 |
| P8 | −2j + j | + 1 | + 2 | | −j + 3 |

**Tab. 3.** Reference pilots.

The estimation is made by sending $N_\mathrm{p}$ repetitions of each pilot. Given the fact that the noise is Gaussian with zero mean, an increase in the number of repetitions $N_\mathrm{p}$, used to compute the average value, minimizes the residual noise contribution in the final result. Regarding the channel, we assume that it remains invariant over the $N_\mathrm{p}$ repetitions of each pilot. The receiver calculates the average of the Euclidean distance between received pilots $p^r_{k,i}$ and $p^r_{p,i}$, through

$$\delta_{k,p} = \frac{\sum_{n=0}^{N_\mathrm{p}} p^r_{k,n} - \sum_{n=0}^{N_\mathrm{p}} p^r_{p,n}}{N} \tag{25}$$

where $N_\mathrm{p}$ is the number of repetitions of each pilot, $k = 1$ and $p = 2, 4, 7, 8$. Without noise we may write

$$\begin{aligned}
\delta_{12} &= \frac{\sum_{n=0}^{N_\mathrm{p}} p_{(1,n)} - \sum_{n=0}^{N_\mathrm{p}} p_{(2,n)}}{N} = 2 = 2g_2^{\mathrm{ref}},\\
\delta_{14} &= \frac{\sum_{n=0}^{N_\mathrm{p}} p_{(1,n)} - \sum_{n=0}^{N_\mathrm{p}} p_{(4,n)}}{N} = 2j = 2g_3^{\mathrm{ref}},\\
\delta_{17} &= \frac{\sum_{n=0}^{N_\mathrm{p}} p_{(1,n)} - \sum_{n=0}^{N_\mathrm{p}} p_{(7,n)}}{N} = 4 = 2g_4^{\mathrm{ref}},\\
\delta_{18} &= \frac{\sum_{n=0}^{N_\mathrm{p}} p_{(1,n)} - \sum_{n=0}^{N_\mathrm{p}} p_{(8,n)}}{N} = 4j = 2g_1^{\mathrm{ref}}
\end{aligned} \tag{26}$$

where $g_i^{\mathrm{ref}}, i = 1, 2, 3, 4$, are the reference coefficients. When noise is present we may write

$$\begin{aligned}
\delta_{12} &= 2 + \varepsilon_{1,2} = 2g_2 = 2g_2^{\mathrm{ref}} \mathrm{e}^{\mathrm{j}\Delta\phi_2},\\
\delta_{14} &= 2j + \varepsilon_{1,4} = 2g_4 = 2g_4^{\mathrm{ref}} \mathrm{e}^{\mathrm{j}\Delta\phi_4},\\
\delta_{17} &= 4 + \varepsilon_{1,7} = 2g_3 = 2g_3^{\mathrm{ref}} \mathrm{e}^{\mathrm{j}\Delta\phi_3},\\
\delta_{18} &= 4j + \varepsilon_{1,8} = 2g_1 = 2g_1^{\mathrm{ref}} \mathrm{e}^{\mathrm{j}\Delta\phi_1}
\end{aligned} \tag{27}$$

where $\varepsilon_{k,p}$ denote the residual noise terms and $g_i = g_i^{\mathrm{ref}} \mathrm{e}^{\mathrm{j}\Delta\phi_i}$ are the received coefficients with $\mathrm{e}^{\mathrm{j}\Delta\phi_i}$ denoting a complex factor due to phase difference between the received coefficient and the reference value. Thus, the obtained coefficients are related to the reference ones, apart from a residual noise term $\varepsilon_{k,p}$, through $g_i = g_i^{\mathrm{ref}} \mathrm{e}^{\mathrm{j}\Delta\phi_i}$, so we may write

$$z_{\theta_i} = \mathrm{e}^{\mathrm{j}\Delta\phi_i} = \frac{\sum_{n=0}^{N_\mathrm{p}} p^r_{k,n} - \sum_{n=0}^{N_\mathrm{p}} p^r_{p,n}}{2N g_i^{\mathrm{ref}}} = \frac{\delta_{k,p}}{2g_i^{\mathrm{ref}}} \tag{28}$$

where $i = 2$ for $k = 1$ and $p = 2$, $i = 4$ for $k = 1$ and $p = 4$, $i = 3$ for $k = 1$ and $p = 7$, and $i = 4$ for $k = 1$ and $p = 8$. It should be mentioned that when the constellations are optimized for an angle $\Phi$, each reference coefficient $g_{iref}$ must be multiplied by a factor $\Delta\Phi$. Next, the phase rotations related with the values computed before, are obtained through

$$\Delta\Phi = \arctan\left(\frac{\mathrm{Re}(z_{\phi_i})}{\mathrm{Im}(z_{\phi_i})}\right). \tag{29}$$

Based on these phase rotations it is possible to obtain the $g_i$ estimates $\hat{g}_i$ using

$$\hat{g}_i = g_i^{\mathrm{ref}} \mathrm{e}^{\mathrm{j}\Delta\phi_i}. \tag{30}$$

Once the coefficients have been estimated, the estimated pilots $P_\mathrm{e}$ are obtained using the product of the Hadamard matrix by the estimated coefficients

$$P_\mathrm{e} = \boldsymbol{H} \cdot \hat{g}_i. \tag{31}$$

The adopted value for $N$ is defined according to a threshold value from which the residual term associated to noise can be scorned. Thus, we may write

$$\boldsymbol{\kappa} \leq \frac{|\boldsymbol{g_i}|^2}{F} \tag{32}$$

where $\boldsymbol{g} = [g_1, g_2, g_3, g_4]$ are the coefficients associated to each amplification branch of the transmitter and $F$ is an attenuation factor. Without compromising complexity, it can be adopted a value $F = 100$, which corresponds to a residual noise term 20 dB below the energy of each of the BPSK component (obviously, this value can be higher or lower depending on the desired system performance in order to avoid a floor effect due to residual noise). Consequently, in the pilots transmission there is a learning phase, since as long as the threshold value established for all coefficients are not reached the process of sending pilots is repeated with an increasing number of pilots $N$. The estimation process is repeated until the condition given by (32) is verified.

### 5.2 Correction of Phase Rotations

With the estimates $\hat{g}_i$ and estimated pilots it is possible to map the new constellation. When it is reached the threshold value, the matrix $\boldsymbol{Z_{16\times16}}$ with all the distance values between the estimated pilot and all constellation symbols is computed (it can be the original constellation or another optimized for an angle $\Phi$) using

$$\boldsymbol{Z_i} = P_\mathrm{e} - P_\mathrm{r} \tag{33}$$

where $P_\mathrm{r}$ denotes the array with the received pilots (the mean of each ones) and $P_\mathrm{e}$ is the array with the estimated pilots. For each symbol the minimum distance of the corresponding symbol of the estimated constellation $\psi'$ is selected, through

$$\psi_i' = \min |\boldsymbol{Z}_i|. \tag{34}$$

When this estimation method or the methods proposed in [27] are adopted the performance results shown previously in Fig. 10 and 11 remain unchanged.

## 6. Combining Two Layers

In previous sections was obvious the security allowed by the layer 1 of the the transmitter, together with the better power efficiency allowed by the multi-branch power amplification. It was also demonstrated that physical security comes without sacrificing the decoding capacity of an authorized user. Despite these positive aspects, it is also important to demonstrate that the combination of layers 1 and 2 does

not cause degradation in performance compared to a system based only on a layer 2 configuration. Thus, it seems crucial to evaluate the impact of combining the two layers in system performance. For that purpose, let us consider the multi-user massive MIMO scenario characterized by the transmission between a BS (Base Station) with $N_t$ antennas and $N_u$ users, each one with $N_r$ receive antennas (obviously we have $N_t \geq N_u \times N_r$ transmit antennas). The channels between each transmit and receive antenna are assumed to be severely time-dispersive and an SC-FDE block transmission technique is employed by each user.

The $t^{th}$ antenna of BS transmits the block of $N$ data symbols $\{x_n^{(t)}; n = 0, 1, \ldots, N-1\}$ being $\{y_n^{(r)}; k = 0, 1, \ldots, N-1\}$ the received block at the $r^{th}$ user antenna (as with other SC-FDE schemes, a cyclic prefix is appended to each transmitted block and removed at the receiver). When appropriate cyclic prefixes sizes are higher than the maximum channel delay spread, the corresponding frequency-domain block $\{Y_k; k = 0, 1, \ldots, N-1\}$ for each user is given by

$$\mathbf{Y}_k = \left[Y_k^{(1)} \ \ldots \ Y_k^{(N_r)}\right]^T = \mathbf{H}_k \mathbf{X}_k + \mathbf{z}_k \tag{35}$$

where $\mathbf{H}_k$ denotes the $N_t \times N_r$ channel matrix for the $k$th frequency, $\mathbf{X}_k = \left[X_k^{(1)} \ldots X_k^{(N_t)}\right]^T$ and $\mathbf{z}_k$ denotes the channel noise. For a linear MMSE-based receiver the data symbols can be obtained from the IDFT of the block $\{\tilde{X}_k^{(N_r)}; k = 0, 1, \ldots, N-1\}$, are

$$\tilde{\mathbf{X}}_k = [\tilde{X}_k^1 \ldots \tilde{X}_k^{(N_r)}]^T = \left(\mathbf{H}_k \mathbf{H}_k^H + \alpha \mathbf{I}\right)^{-1} \mathbf{H}_k^H \mathbf{Y}_k \tag{36}$$

(see details in [19], e.g.), where $\mathbf{I}$ is an appropriate identity matrix and $\alpha = E[|z_k|^2]/E[|X_k^{(N_r)}|^2]$ is assumed identical for all $N_r$ antennas. From (36) becomes evident that complexity of equalization performed at receiver lies on matrix inversion needed for each frequency, and the dimensions of these matrices can be very high in massive MIMO systems. At this time we restrict the iteration number to one (although relevant for system overall performance, the number of iterations is not relevant for comparison purposes between the two transmitter options).

A MMSE precoding technique is adopted to cancel channel interference between users. The system continues to be composed by three main elements, namely the transmitter, the channel $\mathbf{H}$ and the receiver. Since we have $M = N_v \times 16$ antennas at the base station and 2 users, each with single antenna, the resulting channel can be represented as a $2 \times M$ matrix given by

$$\mathbf{H} = \begin{bmatrix} \mathbf{H}_{11} & \mathbf{H}_{12} \\ \mathbf{H}_{21} & \mathbf{H}_{22} \end{bmatrix}$$

where $\mathbf{H}_{11}$,$\mathbf{H}_{12}$, $\mathbf{H}_{21}$ and $\mathbf{H}_{22}$ are $1 \times M$ matrices where each entry $h_{i,j}$ denotes the attenuation and phase shift between the $j^{th}$ transmit antenna and the $i^{th}$ receiver. Due to the symbol interference, in the first user, the received signal by user 1 is given by

$$Y_1 = \mathbf{H_{11}} X_1 + \mathbf{H_{21}} X_2 + \mathbf{z}_1 \tag{37}$$

and, for the user 2 we have

$$Y_2 = \mathbf{H_{12}} X_1 + \mathbf{H_{22}} X_2 + \mathbf{z}_2 \tag{38}$$

with $\mathbf{z}_1$ and $\mathbf{z}_2$ being AWGN noise on the first and second user's receiver, respectively and $X_1$ and $X_2$ are the frequency domain blocks of the data blocks associated to each user. Adopting the matrix notation it is possible to write

$$\begin{bmatrix} Y_1 \\ Y_2 \end{bmatrix} = \begin{bmatrix} \mathbf{H}_{11} & \mathbf{H}_{12} \\ \mathbf{H}_{21} & \mathbf{H}_{22} \end{bmatrix} \begin{bmatrix} X_1 \\ X_2 \end{bmatrix} + \begin{bmatrix} \mathbf{z}_1 \\ \mathbf{z}_2 \end{bmatrix}$$

and therefore we may write

$$Y = \mathbf{H}X + \mathbf{z}. \tag{39}$$

Since it is assumed perfect CSI, $\mathbf{H}$ is known. To solve previous equation for x, we need to find the precoding matrix $\mathbf{W}$ which satisfies $\mathbf{WH} = \mathbf{I}$, with $\mathbf{I}$ representing the identity matrix. The solution is given by:

$$\mathbf{W} = \beta \mathbf{H}^{-1}, \tag{40}$$

with

$$\beta = \sqrt{\frac{M}{T(\mathbf{H}^{-1}(\mathbf{H}^{-1})^H)}} \tag{41}$$

and

$$\mathbf{H}^{-1} = \mathbf{H}^H (\mathbf{H}\mathbf{H}^H + \frac{\sigma_z^2}{\sigma_x^2}\mathbf{I})^{-1} \tag{42}$$

where $(.)^H$ denotes the Hermitian transpose.

## 6.1 Simulation Results

Regarding the transmitter configuration we consider two different options as in [28]. In the first one, it is based on the layered transmitter structure shown previously in Fig. 1, but where both layers 1 and 2 are used. Layer 1, is composed by the $N_v$ amplification branches in parallel (for 16-QAM and 64-QAM we have $N_v = 4$ and $N_v = 6$, respectively), with each one connected to an horizontal array with $N_h = 16$ that composes the second layer. This means that we have info directivity due to constellation shaping combined with horizontal beamforming achieved by each array of 16 antennas connected to each amplifier. In the second option, the transmitter uses only one amplification branch connected to a bi-dimensional antenna array with $N_u \times N_b$ elements, which is the conventional approach where the same constellation symbol is transmitted by all antennas. Hence, in the first option info directivity due to constellation shaping is combined with the horizontal spatial directivity caused by each horizontal array of 16 antennas. In the second option the array with $N_v \times 16$ antennas optimizes the horizontal and vertical directivities of the beam to the direction of the intended user.

Both options may have two arrays configurations with different vertical spacings $d_v$ between antennas of $\lambda$ or $\lambda/4$ (the second value corresponds to the uniform configuration

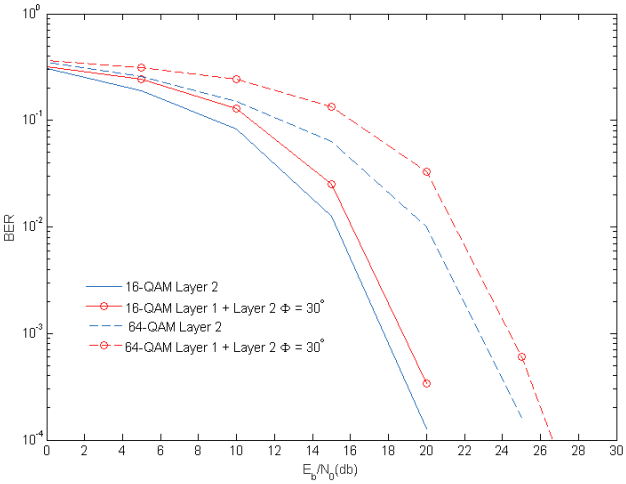


**Fig. 12.** BER for both transmitter options in a multi-user scenario with an angular separation of 12° between users and $d_v = \lambda/4$.

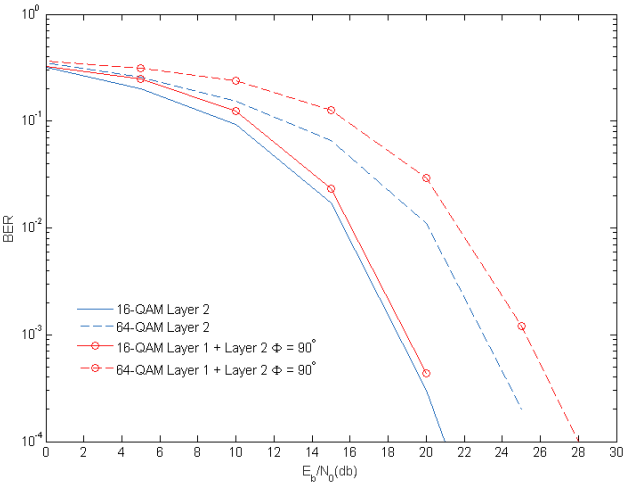


**Fig. 13.** BER for both transmitter options in a multi-user scenario with an angular separation of 12° between users and $d_v = \lambda$.

already analyzed in Sec. 3.1) and in the horizontal plane the antennas are always spaced by $\frac{1}{2}\lambda$ (in this case it is achieved a radiation pattern with a main lobe angular width of 8° and second lobes with an attenuation of 12 dBs). Since we have different vertical spacings the angles $\Phi$ in which the constellation is optimized by layer 1 also vary. This means that we assume $\Phi = 30°$ when the vertical spacing is $\lambda/4$ and $\Phi = 90°$ for a vertical spacing of $\lambda$. It is also assumed that each $N_v \times 16$ array patch at the BS serves a single user with one receive antenna and only two users are considered. It is also assumed a spacing between the two users that leads to an angular separation between the radiation beams of $\theta = 12°$. For the sake of simplicity, we assume an uniform PDP, with 4 sets of 8 equal-power taps, with uncorrelated Rayleigh fading on each tap (note that power varies with the arrival angle due to directive radiation beam) and uncorrelated between the two antenna patches. Again, the transmitted symbols $s_n$ are selected with equal probability from a $M$-QAM constellation (dimensions of $M = 16$ and $M = 64$ are considered). It is assumed that the receiver knows the set of coefficients $g_i$ used in layer 1. The other simulation conditions are the same adopted in Sec. 4.

In Fig. 12 and 13 we present the BER results for $d_v = \lambda/4$ and $d_v = \lambda$, respectively. From the results of Fig. 12 and 13 it is clear that the increased power efficiency and constellation shaping of the layer 1 comes with a very low impact on performance, since results show that both transmitter configurations have similar performances. It can be seen that massive MIMO implementations using the combination of layer 1 with layer 2, do not compromise the BER performance since the impact is less than 1 dB for vertical spacings of $\lambda/4$ and less than 0.25 dB for 16-QAM with vertical spacing of $\lambda$. Only for 64-QAM with $d_v = \lambda$ the impact on performance is higher than 1 dB, but the increase on power amplification efficiency can easily surpass this degradation and other angles leading to better performance may be considered. This means that power efficient structure of layer 1 can be adopted without sacrificing system performance, since the absence of power directivity in the vertical plane has a very small influence on the overall system performance. Hence, the constellation shaping of layer 1 can be used for physical layer security together with beamforming with comparable performance of classical implementation where all antennas of layer 2 are used for directivity purposes.

Having in mind these aspects it seems obvious that shaping of the constellation achieved by this transmitter structure can be used to implement security at physical level, wile the energy efficiency of power amplification is increased due to the use of saturated amplifiers.

## 7. Conclusions

In this paper it was shown that a transmitter based on a double layer structure with information directivity and horizontal beamforming achieves practically the same performance of common beamforming (based on a 2-D array). It became obvious that a multi layer transmission structure can be used to achieve better power efficiency and physical layer security together with Layer 2 in massive MIMO implementations. The layer 1 based on multilevel modulations decomposition as a sum of BPSK components, introduces channel security at the physical layer without sacrifice of the spectral and BER performance. The BER results achieved by both options are similar, but overall energy system efficiency can be higher in a double layer system since the amplification is done with saturated amplifiers.

## Acknowledgments

This work was supported in part by CTS multi-annual funding project PEst-OE/EEI/UI0066/2014 (UNINOVA),IT UID/EEA/50008/2013 (plurianual founding and project GLANCES), EnAcoMIMOCo EXPL/EEI-TEL/2408/2013, project IT UID/EEA/50008/2013 - MM5G and Program Investigador FCT under Grant IF/00325/2015.

# References


[1] RUSEK, F., PERSSON, D., LAU, B. K., et al. Scaling up MIMO: Opportunities and challenges with very large arrays. *IEEE Signal Processing Magazine*, 2013, vol. 30, no. 1, p. 40–60. DOI:10.1109/MSP.2011.2178495

[2] BOCCARDI, F., HEATH JR., R. W., LOZANO, A., et al. Five disruptive technology directions for 5G. *IEEE Communications Magazine*, 2014, vol. 52, no. 2, p. 74–80. DOI: 10.1109/MCOM.2014.6736746

[3] NGO, H. Q., LARSSON, E. G., MARZETTA, T. L. Energy and spectral efficiency of very large multiuser MIMO systems. *IEEE Transactions on Communications*, 2013, vol. 61, no. 4, p. 1436–1449. DOI: 10.1109/TCOMM.2013.020413.110848

[4] GERSHAM, A. B., SIDIROPOULOS, N. D., SHAHBAZPANAHI, S. Convex optimization-based beamforming. *IEEE Signal Processing Magazine*, 2010, vol. 27, no. May, p. 62–75. DOI: 10.1109/MSP.2010.936015

[5] LI, W., CHANG, T., LIN, C., et al. Coordinated beamforming for multiuser MISO interference channel under rate outage constraints. *IEEE Transactions on Signal Processing*, 2013, vol. 61, no. 5, p. 1087–1103. DOI: 10.1109/TSP.2012.2231080

[6] WANG, R., CAI, J., YU, X., et al. Disruptive technologies and potential cellular architecture for 5G. *Open Electrical Electronic Engineering Journal*, 2015, no. 9, p. 512–517. DOI: 10.2174/1874129001509010512

[7] ASTUCIA, V., MONTEZUMA, P., DINIS, R., et al. On the use of multiple grossly nonlinear amplifiers for higly efficient linear amplification of multilevel constellations. In *Proceedings of the IEEE Vehicular Technology Conference (VTC) 2013-Fall*. 2013, p. 1–5. DOI: 10.1109/VTCFall.2013.6692320

[8] MONTEZUMA, P., GUSMÃO, A. Design of TC-OQAM schemes using a generalised nonlinear OQPSK-type format. *IEE Electronics Letters*, 1999, vol. 35, no. 11, p. 860–861. DOI: 10.1049/el:19990616

[9] MONTEZUMA, P., DINIS, R. Implementing physical layer security using transmitters with constellation shaping. In *Proceedings of the IEEE International Conference on Computer Communications and Networks (ICCCN) 2015*. 2015, p. 1–4. DOI: 10.1109/ICCCN.2015.7288418

[10] FERREIRA, A. Massive MIMO Transmission Techniques. (Master Thesis). FCT, UNL, Lisbon, Sep. 2016.

[11] DINIS, R., MONTEZUMA, P., SOUTO, N., et al. Iterative frequency-domain equalization for general constellations. In *Proceedings of the IEEE Sarnoff Symposium*. 2010, p. 1–5. DOI: 10.1109/SARNOF.2010.5469792

[12] AMOROSO, F., KIVETT, J. Simplified MSK signalling technique. *IEEE Transactions on Communications*, 1977, vol. 25, no. 4, p. 433–441. DOI: 10.1109/TCOM.1977.1093835

[13] BEKO, M., DINIS, R. Designing good multi-dimensional constellation. *IEEE Wireless Communications Letters*, 2012, vol. 1, no. 3, p. 221–224. DOI: 10.1109/WCL.2012.032312.120203

[14] BARICZ, Á. *Generalized Bessel Functions of the First Kind*. Springer, 2010. DOI: 10.1007/978-3-642-12230-9

[15] CAIRE, G., TARICCO, G., BIGLIERI, E. Bit-interleaved coded modulation. *IEEE Transactions on Information Theory*, 1998, vol. 44, p. 927–947. DOI: 10.1109/18.669123

[16] XU, Z., YUAN, T., GONG, Y., et al. Achieving secure communication through random phase rotation technique. In *IEEE Wireless Communications and Mobile Computing Conference (IWCMC)*. 2017, p. 2073–2078. DOI: 10.1109/IWCMC.2017.7986603

[17] BENVENUTO, N., TOMASIN, S. Block iterative DFE for single carrier modulation. *IEE Electronics Letters*, 2002, vol. 39, no. 19, p. 1144–1145. DOI: 10.1049/el:20020767

[18] DINIS, R., KALBASI, R., FALCONER, D., et al. Iterative layered space-time receivers for single-carrier transmission over severe time-dispersive channels. *IEEE Commmunications Letters*, 2004, vol. 8, no. 9, p. 579–581. DOI: 10.1109/LCOMM.2004.835339

[19] SILVA, P., DINIS, R. *Frequency-Domain Multiuser Detection for CDMA Systems*. River Publishers, 2012. ISBN: 9788792329707

[20] SILVA, F., DINIS, R., MONTEZUMA, P. Estimation of the feedback reliability for IB-DFE receivers. *International Scholarly Research Notices Communications and Networking*, 2011, vol. 2011, p. 1–7. DOI: 10.5402/2011/980830

[21] MASSEY, J. L. An introduction to contemporary cryptology. *Proceedings of the IEEE*, 1988, vol. 76, no. 5, p. 533–549. DOI: 10.1109/5.4440

[22] BARENGHI, A., BREVEGLIERI, L., KOREN, I., et al. Fault injection attacks on cryptographic devices: Theory, practice, and countermeasures. *Proceedings of the IEEE*, 2012, vol. 100, no. 11, p. 3056–3076. DOI: 10.1109/JPROC.2012.2188769

[23] HARRISON, W. K., ALMEIDA, J., BLOCH, M. R., et al. Coding for secrecy: An overview of error-control coding techniques for physical-layer security. *IEEE Signal Processing Magazine*, 2013, vol. 30, no. 5, p. 41–50. DOI: 10.1109/MSP.2013.2265141

[24] COLERI, S., ERGEN, M., PURI, A., et al. Channel estimation techniques based on pilot arrangement in OFDM systems. *IEEE Transactions on Broadcast*, 2002, vol. 48, no. 3, p. 223–229. DOI: 10.1109/TBC.2002.804034

[25] HSIEH, M. H., WEI, C. Channel estimation for OFDM systems based on comb-type pilot arrangement in frequency selective fading channels. *IEEE Transactions on Consumer Electronics*, 1998, vol. 44, no. 1, p. 217–225. DOI: 10.1109/30.663750

[26] MANGQING, G., GANG, X., JINCHUN, G., et al. Enhanced EVD based channel estimation and pilot decontamination for massive MIMO networks. *Journal of China Universities Posts and Telecommunications*, 2015, vol. 22, no. 6, p. 72–77. DOI: 10.1016/S1005-8885(15)60697-5

[27] MONTEZUMA, P., DINIS, R., RIBEIRO, S., et al. Two methods for estimation of amplifier imbalances in multi-amplifier transmission structures. *Radioengineering*, 2017, vol. 26, no. 1, p. 285–290. DOI: 10.13164/re.2017.0285

[28] FERREIRA, A., GASPAR, G., MONTEZUMA, P., et al. Combining info and spatial directivities in multiple antenna transmission systems. In *IEEE Young Engineers Forum (YEF-ECE) 2017*. 2017, p. 1–5. DOI: 10.1109/YEF-ECE.2017.7935631


# About the Authors ...

**Paulo MONTEZUMA** received his PhD from FCT-Universidade Nova de Lisboa. He has been actively involved in several international research projects in the broadband wireless communications area and many national projects. His main research activities are on modulation and transmitter design, coding, nonlinear effects on digital communications and receiver design, with emphasis on frequency-domain implementations, namely for single carrier and multi-carrier modulations.

**Rui DINIS** received the Ph.D. degree from Instituto Superior Tecnico (IST), Technical University of Lisbon, Portugal, in

2001 and the Habilitation in Telecommunications from Faculdade de Ciencias e Tecnologia (FCT), Universidade Nova de Lisboa (UNL), in 2010. His main research activities are on modulation and transmitter design, signal processing, nonlinear effects on digital communications and receiver design, with emphasis on frequency-domain implementations, namely for MIMO systems and/or OFDM and SC-FDE modulations.

**Afonso FERREIRA** received the M.Sc degree from from Faculdade de Ciencias e Tecnologia (FCT), Universidade Nova de Lisboa (UNL), in 2016. His main research activities are on multi-antenna transmitter design, OFDM and SC-FDE modulations.

**Marko BEKO** was born in Belgrade, Serbia, on November 11, 1977. He received the Dipl. Eng. degree from the University of Belgrade, Belgrade, Serbia, in 2001 and the PhD degree in electrical and computer engineering from Instituto Superior Tecnico, Lisbon, Portugal, in 2008. Currently, he is an Associate Professor at the Universidade Lusófona de Humanidades e Tecnologias, Portugal. He is also a Researcher at the UNINOVA, Campus da FCT/UNL, Monte de Caparica, Portugal. His current research interests are in the area of signal processing for wireless communications and nonsmooth and convex optimization. He is the winner of the 2008 IBM Portugal Scientific Award.